

Influence of stress concentrator shape and testing temperature on impact fracture regularities of pipeline steel

I V Vlasov^{1,3}, S V Panin^{1,3}, P O Maruschak², D D Moiseenko¹ and F Berto⁴

¹ Institute of Strength Physics and Materials Science RAS, 2/4, pr. Akademicheskii, Tomsk, 634021, Russia

² Ternopil Ivan Puluj National Technical University, 56, str. Ruska, Ternopil, 46001, Ukraine

³ National Research Tomsk Polytechnic University, 30, Lenina ave. Tomsk, 634050, Russia

⁴ NTNU, Department of Engineering Design and Materials, 7491, Richard Birkelands vei 2b, Trondheim, Norway

E-mail: maruschak.tu.edu@gmail.com

Abstract. The structure and impact toughness of the pipeline 17Mn1Si steel have been studied. The main attention was paid to the analysis of various conditions of stress concentration under dynamic loadings. The process of strain localization with increasing stress state stiffness at the tip of the concentrator with decreasing testing temperature was investigated. Impact loading diagrams for specimens with various stress concentrator shapes were registered and analyzed.

1. Introduction

Increasing service life time of structural elements is one of the most difficult and actual requirements for transportation engineering. Recently, an intensive building and renovation of existing oil and gas pipelines takes place. During operation, the pipe material experiences pressure drops, strain aging, corrosion, abrasion, etc. [1] Large oil and gas deposits to be excavated in the north conditions make the problem more complex due to operation at negative temperatures [2]. In this regard, the actual problem is to improve the operational properties of pipe steel by providing higher mechanical properties [3]. One of the most common and well-standardized methods for mechanical properties certification of pipe steel is the impact testing [4, 5].

Pipe steels are characterized by high values of impact toughness. This is related to the fact that one should diminish the risk of accidental failures of the pipe under pressure as well as reduce the impact of the mechanical properties dispersion and presence of manufacturing defects induced during the steel production [6, 7]. Thus, the assessment of the influence of defects and structure heterogeneity of pipe steel by varying the shape of stress concentrators, especially its radius is of particular importance [5-8]. The data of this kind will allow taking into account the embrittlement factors that influence the stability of pipe steel to impact deformations.

An important task is also the study of fracture mechanisms at different stress stiffness values. Its importance is governed by practical applications associated with the interpretation of elastic-plastic characteristics of fracture resistance of structural materials in the presence of service defects [1].

This paper studies the influence of the notch shape on the impact fracture of 17Mn1Si steel at different, first of all, negative temperatures.

2. Experimental

Specimens for investigation were spark cut out of a pipe steel sheet of 30 mm thickness produced at the Machine Building Factory of Yurga (Russia). A batch of specimens with V-, U- and I-shaped



notches of equal depth (2 mm) was machined. V- and U-notches were made by standard milling cutters; I-notches were made by electroerosion. Notch tip radius: U-1.0 mm; V-0.25 mm; I-0.1 mm. Before low-temperature impact loading the specimens were kept in a refrigerator (cooling chamber) 'Lauda rp870' for 10 minutes in the temperature range from $-60\text{ }^{\circ}\text{C}$ to $0\text{ }^{\circ}\text{C}$. The time interval between the specimen extraction from the cooling chamber and further testing did not exceed 5 seconds. At least three specimens of each type were tested at temperatures $20, 0, -20, -40$ and $-60\text{ }^{\circ}\text{C}$ on an impact pendulum Instron 450MPX with recording the impact diagram, Table 1. The data processing program divides the specimen fracture energy into two constituents, such as load-time ($P-t$) and load-curvature ($P-s$). The deformation and fracture mechanisms were studied by fracture surface images using a scanning electron microscope LEO EVO 50 (Zeiss, Germany).

3. Results and Discussion

Metallography. Specimens for testing had the ferrite-pearlite structure with an average grain size of $14.7 \pm 2.5\ \mu\text{m}$ (figure 1). Ferrite grains had predominantly globular shape which is typical for 17Mn1Si steel. The high content of ferrite phase provides greater fracture toughness that is of particular importance under dynamic loading. Higher strength of the pearlite phase ensures possessing appropriate mechanical properties being required for the pipe operation under exploitation pressure.

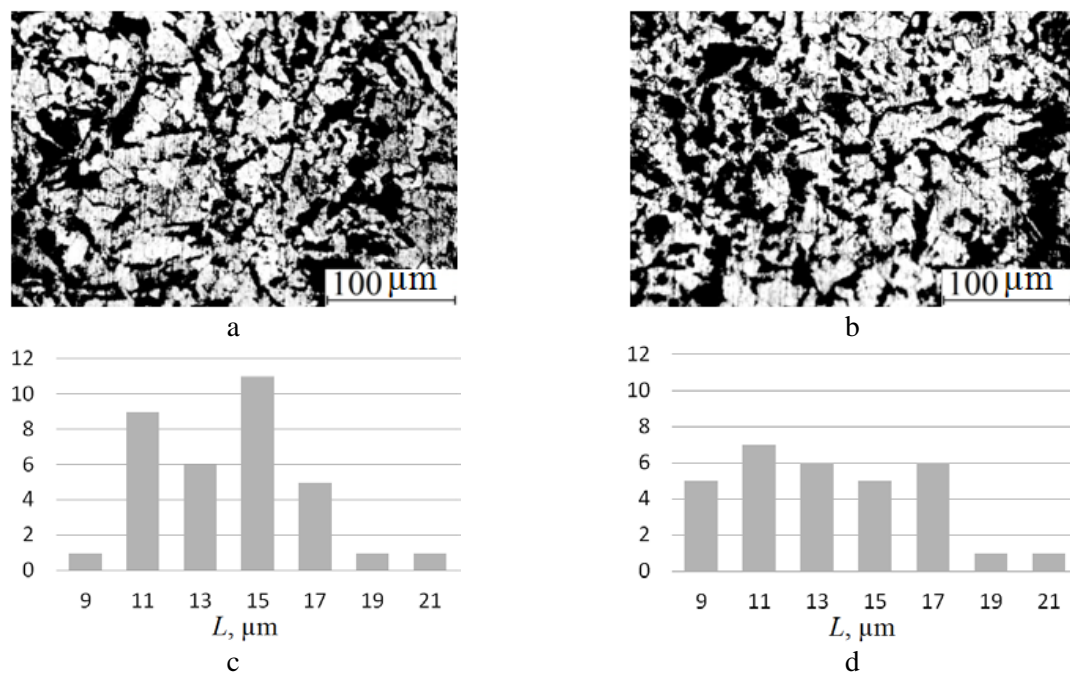


Figure 1. Optical micrographs of the 17Mn1Si steel in the supplied state (a, b); grain size distribution histograms along vertical (c) and horizontal (d) directions

Fracture macromechanisms. The test temperature dependence of impact toughness (figure 2, a, Table 1) exhibits several portions [9]. On the first portion (from $T = -60\text{ }^{\circ}\text{C}$ to $T = -40\text{ }^{\circ}\text{C}$), the specimen fracture is brittle, without pronounced signs of plastic deformation. The test temperature growth up to $-20\text{ }^{\circ}\text{C}$ triggers combined fracture mechanisms. The third portion (from $0\text{ }^{\circ}\text{C}$ to $20\text{ }^{\circ}\text{C}$) corresponds to the region of ductile fracture characterized by plastic flow on both the micro- and macroscale. The literature data [9, 10] indicate that each portion corresponds to certain fracture micromechanisms.

Let us note that the form of the obtained impact toughness dependences for specimens with sharp V- and I-notches almost coincide within the entire studied temperature range. An exception is the temperature $-20\text{ }^{\circ}\text{C}$ at which the impact toughness of V-notched specimens is slightly higher than that

of I-notched specimens. On the whole, the impact toughness of U-notched specimens is about 3 times higher in the entire test temperature range than that of V-notched specimens (figure 2). It can be assumed in a certain approximation that the impact toughness value for specimens with all three types of notches linearly decreases with the decreasing test temperature.

The obtained dynamic loading curves of the specimens corroborate their sensitivity to changes in the macrofracture localization conditions which are associated with the changed concentrator shape (figure 2). It can be said in general that the curve shape is typical of ductile fracture within the entire studied temperature range from 20 °C to –60 °C [11], as well as for specimens with sharper V- and I-notches. The form of the impact diagrams of the V- and I-notched specimens is almost the same, which indicates that crack initiation and growth occur at similar stages. Let us consider them in more detail.

V-notch. Specimens of 17Mn1Si steel fracture in a ductile manner at test temperatures from 20 °C to –20 °C, which is evidenced by gently ascending and descending curve portions (figure 2, b–d, curve KCV). The microscale deformation mechanisms allow effective stress relaxation [12]. The crack initiation and growth take place in a “classical” manner, i.e., consecutively, without interruption and abrupt bifurcation transitions. The material shows high ductility and crack resistance. At the test temperatures –40 °C and –60 °C, the fracture diagram narrows and peaks. The form of the descending curve portion points to brittle crack propagation [12]. This is especially typical of the test temperature $T = -60$ °C at which the maximum load decreases down to $P_{\max} = 7$ kN, which is indicative of a partial loss of the bearing capacity of the material [13].

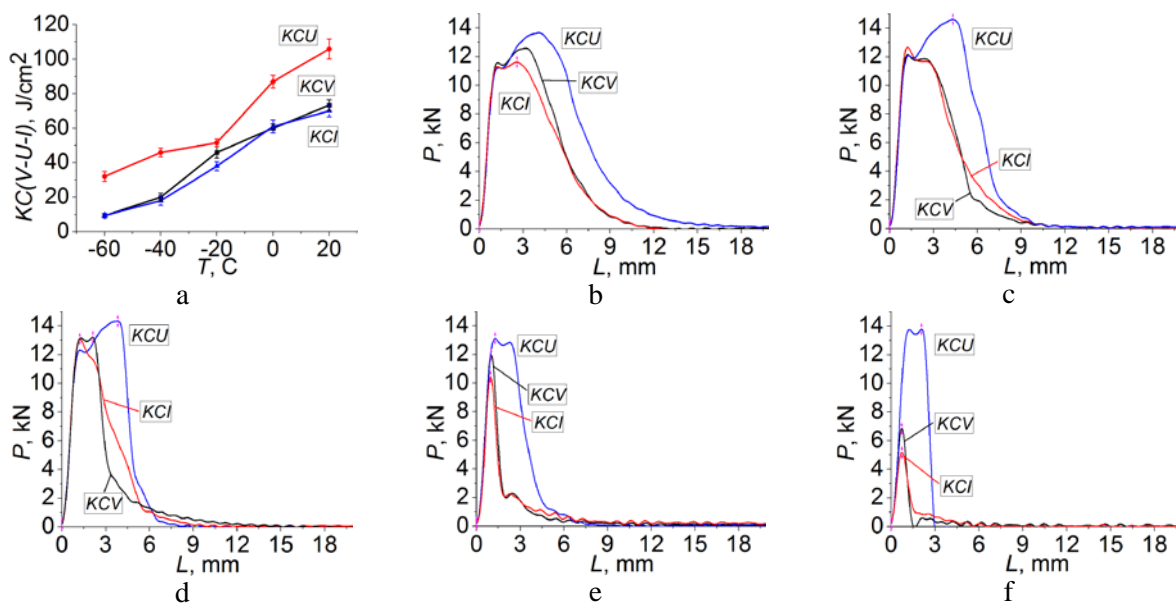


Figure 2. Test temperature dependence of impact toughness (a); impact diagrams in the load/displacement coordinates at test temperatures: 20 °C (b); 0 °C (c); –20 °C (d); –40 °C (e); –60 °C (f) for V-, U- and I-notched specimens.

I-notch. The form of the loading diagram (figure 2, b–f, curve KCI) is similar to that of the V-shaped concentrator (figure 2, b–f). Hence, with the sharpest concentrator (compared to the V-notch; notch tip radius is 0.25 and 0.1 mm, respectively) the fracture behavior of the material does not appear to be more brittle, even in the case of such a sharp notch similar in shape to a fatigue crack. In our opinion, this is due to the fact that plastic deformation ahead the tip of the main crack during its propagation in the studied steel provides for partial stress relaxation.

The influence of the test temperature reduction for the I-notched specimens is similar to the influence described above for the V-notched specimens. At $T = -60$ °C the maximum load value

decreases even more abruptly down to $P_{max} = 5$ kN. This is testimony to a more pronounced embrittling effect of the concentrator, which corresponds well to the minimum notch tip radius.

U-notch. The impact fracture of notched 17Mn1Si steel specimens with the maximum notch tip radius is accompanied by ductile deformation. The observed macroscopic deformation behavior of the material bears witness to the activation of relaxation processes, which leads to an increase in the height and width of the impact diagram in the entire studied temperature range.

As one can see, the maximum load value decreases at room temperature (figure 2, b) with the growing stress concentration at the notch tip (in transition from the U- to I-notch). The height of the yield point increases in this case and its peak in the I-notched specimen corresponds to maximum load P_{max} . Thus, an increase in the material volume involved in deformation resistance, like for the U-notch due to its larger area and larger radius, increases resistance to macrocrack initiation and growth. However, this occurs at lower values of load P at the stage of elastic deformation as compared to the case of the I-shaped notch.

The yield plateau in the impact diagrams of I-notched specimens is little pronounced, 'degenerated'. This is testimony to the occurrence of local hardening processes on early deformation stages, which is accompanied by a decrease in the resistance of steel to strain localization in bending (this is dangerous for pipelines).

Integral estimation of impact diagrams. From the viewpoint of experimental data application, one of the most important issues in post-critical deformation models is the determination of the point of transition to the post-critical stage of specimen deformation, i.e., the stage of crack growth. Table 1 contain the force and energy parameters of impact toughness for 17Mn1Si steel. Like in our previous papers [1, 12], we may assume the maximum load in impact testing P_{max} as the macrocharacteristic that reflects the material strength.

Table 1. Maximum load values on impact diagrams.

T, °C	V-notch		U-notch		I-notch	
	KCV, J/cm ²	P_{max} , kN	KCU, J/cm ²	P_{max} , kN	KCI, J/cm ²	P_{max} , kN
-60	9.3±1.1	6.8±0.2	32±2.8	13.8±1.7	9.4±1.3	5.2±0.1
-40	20±2.3	12±1.03	46±2.5	13.1±1	18±2.7	10.4±0.8
-20	46±3.4	13.2±1.01	51.6±2.2	14.3±0.6	38±2.6	13.1±1.3
0	60±2.6	12.2±1.02	87±3.9	14.6±1.4	61±3.7	12.7±1.2
20	73.3±3.2	12.6±2.3	106±5.7	13.7±1.3	70±3.4	11.6±1.5

These data are very important for understanding the effect of stress stiffness on the crack resistance of 17Mn1Si steel because P_{max} corresponds to the point of transition from macrocrack initiation to its propagation. The sharper is the concentrator, the lower is the value of parameter P_{max} at which the crack grows, which is indicative of a stiffer stress state at the crack tip [12].

Macroanalysis of fracture surface morphology. Analysis of laboratory and full-scale pneumatic test data has shown that the capability to arrest extended ductile fracture is determined by the volume and intensity of metal plastic deformation ahead the propagating crack tip [4]. In so doing, the volume of plastically deformed metal ahead the crack tip on the stage of stable ductile crack growth remains almost unchanged [4]. The larger volume is involved in plastic deformation near the propagating crack and the higher is the deformation intensity, the shorter is the fracture length. Thus, an increase in the fracture toughness, first of all, its constituent responsible for the crack growth energy, as well as the presence of plastic strains contractions along the crack front in Charpy specimens are additional factors attesting to high mechanical properties of pipe steel [14].

$T = 20$ °C (for V-, U-, I-notches). The crack initiation zone (zone I) is characterized by transition from the notch at an oblique angle, which points to the presence of macro- and microplastic strains and is confirmed by the shape of shear lips (figure 3, a–c). The fracture surface (zone II) has the form typical of shear rupture. This bears witness to the formation of a plasticity zone ahead the notch tip

and to a heterogeneous stress-strain state in the specimen at crack initiation and growth. In this case, fracture is determined by the inhomogeneity of energy absorption in different specimen regions, particularly, in the zone of shear lips (zone III), which is manifested in the generation of different fracture growth mechanisms and in final specimen rupture (zone IV).

$T = -20\text{ }^{\circ}\text{C}$ (for V-, U-, I-notches). The influence of the plastic deformation processes decreases, which affects the external view of the specimen fracture surfaces (figure 3, d–f). The crack initiation and crack growth zones (zones I and II) formed in a ductile manner, with local regions of plastic deformation. The fracture surface profile takes on the form typical of cleavage fracture (direct fracture). The fracture surface structure exhibits cleavages that lead to plastic strain localization through multiple necking, and thus the volume of plastically deformed metal decreases, including the zones of shear lips (zone III) and final specimen rupture (zone IV).

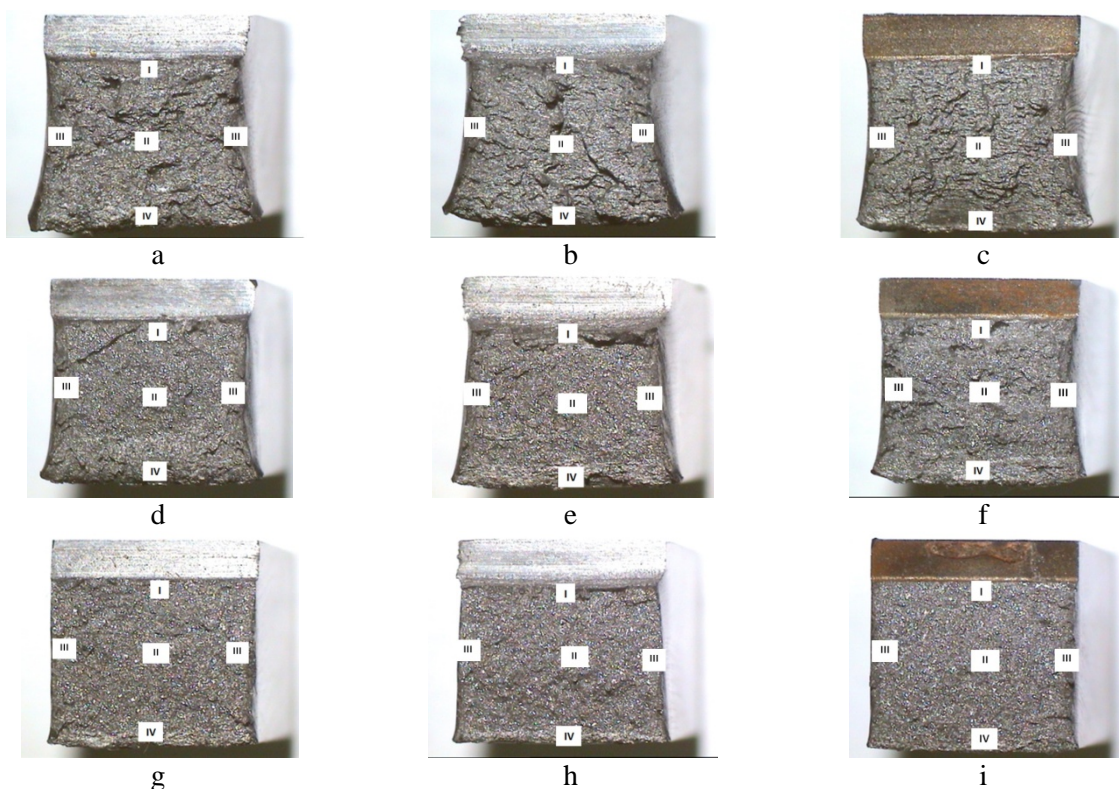


Figure 3 Macrofractures of impact test specimens at different temperatures with the designation of zones: I) – crack initiation; II) - crack growth; III) – shear lips; IV) – final rupture; a), b), c) $T=20\text{ }^{\circ}\text{C}$; d), e), f) $T=-20\text{ }^{\circ}\text{C}$; g), h), i) $T=-60\text{ }^{\circ}\text{C}$; a), d), g) V-notch; b), e), h) U-notch; c), f), i) I-notch.

$T = -60\text{ }^{\circ}\text{C}$ (for V-, U-, I-notches). The regions of crack initiation (zone I) and growth (zone II) exhibit flat surfaces without visible signs of material tear outs at the macroscale. This means that crack propagation along the entire front occurred in stationary conditions, i.e., in nearly the same stress-strain state along the entire front (figure 3, g–i). In this case, crack initiation corresponded to the transition of material to the nonequilibrium state. Fracture in this zone is brittle. The strain rates, shear strain and tangential stress values exerted almost no effect on fracture micromechanisms. We shall notice that the fracture surface of all concentrators in specimens is flat (on the macroscale) with a small zone of shear lips (zone III). This indicates that the stress and strain fields were symmetric relative to the notch and initiated crack as well as during crack propagation and final rupture (zone IV).

The performed tests have shown that with the increasing stress stiffness induced by temperature reduction and strain localization [15], the material approaches a more brittle state and hence its fracture energy decreases.

4. Conclusion

The structure of the 17Mn1Si steel as well as micro- and macroscale mechanisms of its impact fracture in the temperature range of -60 °C – 20 °C have been studied. The main regularities of the notch shape influence onto impact failure energy as well as the form of the loading diagram were revealed. The discussion and generalization of the obtained results have been conducted.

Acknowledgments

The work was performed in the framework of fundamental research projects of the Russian State Academies of Sciences (2013–2020), with a partial support of RFBR Grant No. 15-08-05818_a, and Project of the Headquarter of the Russian Academy of Sciences on Arctic research.

The authors are grateful to Shared Use Center 'Nanotech' of ISPMS SB RAS for the assistance in fractographic investigations.

References

- [1] Maruschak P, Bishchak R, Prentkovskis O, et al 2016 *Adv. in Mech. Eng.* **8(4)** 1-8
- [2] Kontorovich A E, Ermilov O M, Laperdin A N 2013 *Herald of the Russian Academy of Sci.* **83(5)** 400-410
- [3] Arabei A B, Pyshmintsev I Yu, Farber V M, Khotinov V A, Struin A O 2012 *Steel in Translation* **42(3)** 212-218
- [4] Hwang B, Kim Y G, Lee S, Kim N J, Yoo J Y 2005 *Metall. Mater. Trans.* 36A 371-87
- [5] Kudrya A V, Kuz'ko E I, Sokolovskaya E A 2014 *Russian J. Metallurgy* **10** 837-845
- [6] Oh C-K, Kim Y-J, Baek J-H, Kim Y-P, Kim W 2007 *Int. J. of Mech. Sci.* **49(12)** 1399-1412
- [7] Pyshmintsev I Yu, Arabei A B, Farber V M, Khotinov V A, Lezhnin N V 2012 *The Physics of Metals and Metallography* **113(4)** 411-417
- [8] Hashemi S H 2009 *Int.l J. of Pressure Vessels and Piping* **86 (8)** 533-540
- [9] Kotrechko S A, Meshkov Yu Ya 2001 *Strength of Materials* **33(4)** 356-361
- [10] Hashemi S H, Mohammadyani D, Pouranvari M, Mousavizadeh S M 2009 *Fatigue & Fracture of Engin. Materials & Structures* **32** 33-40
- [11] Venkatsurya P K C, Misra R D K, Mulholland M D, Manohar M, Hartmann J E 2014 *Metallurgical and Materials Transactions A* **45(5)** 2335-2342
- [12] Maruschak P O, Danyliuk I M, Bishchak R T, Vuherer T 2014 *Central European J. of Eng.* **4(4)** 408-415
- [13] Sih G C, Tzou D Y 1986 *Theoretical and Applied Fracture Mech.* **5(3)** 189-203
- [14] Xiao-Long Yang, Yun-Bo Xu, Xiao-Dong Tan, Di Wu 2014 *Materials Sci. and Eng.: A* **607(23)** 53-62
- [15] Kazberuk A, Savruk M P, Chornenkyi A B 2016 *Int. J. of Solids and Structures* **85(86)** 134-143